FEATURE ARTICLE

Journal of Materials Chemistry
www.rsc.org/materials

Biotechnological application of nano-scale engineered bacterial magnetic particles

Tadashi Matsunaga,* Yoshiko Okamura and Tsuyoshi Tanaka

Department of Biotechnology, Tokyo University of Agriculture and Technology, 2-24-16 Naka-Cho, Koganei, Tokyo, Japan. E-mail: tmatsuna@cc.tuat.ac.jp; Fax: 81-42-385-7713; Tel: +81-42-388-7020

Received 31st March 2004, Accepted 27th April 2004
First published as an Advance Article on the web 15th June 2004

Magnetic particles have been studied with much interest with reference to many engineering applications. Much effort has been devoted to the preparation of nano-sized magnetite particles with well-controlled size and shape. Magnetic bacteria synthesize uniform and nano-sized magnetite particles enveloped by organic lipid membranes. This review discusses recent advances in bacterial magnetite particles. Especially, the tremendous biotechnological potential of bacterial magnetite particles (BMPs) and our recent understanding of mechanism of magnetite particle formation in *Magnetospirillum magneticum* strain AMB-1 were highlighted.

Introduction

Magnetic particles have utility in practical applications, such as magnetic carriers in immunoassays and drug delivery system, and magnetic memory in electronic applications. Nano-sized magnetite particles have been synthesized by a coprecipitation method with the simplest way *i.e.* coprecipitation of Fe(II) and Fe (III) in alkaline solution.

$$Fe^{2+} + 2Fe^{3+} + 8OH^- \rightarrow Fe_3O_4 + 4H_2O$$

However, preparation of fine magnetite particles by present techniques requires strict control of pH or/and temperature in the reaction process. Much effort has been devoted to the preparation of nano-sized magnetite particles with well-controlled size and shape.

Magnetic bacteria (Fig. 1) synthesize more uniform magnetic particles, which consist of magnetite (Fe_3O_4) and/or greigite (Fe_3S_4),[1–3] in size and shape compared with artificial magnetite particles. The magnetic particles are aligned in chains parallel to the cell axis. Each particle possesses a magnetic dipole moment and magnetic interactions between magnetic particles in a chain are oriented parallel to each other along the chain. Thus, the cell obtains a great deal of magnetic dipole moment enabling the bacterium to sense and migrate along the Earth's geomagnetic field lines and to maintain its position within the boundary of the oxic-anoxic transition zone.[4]

Bacterial magnetite particles (BMPs) are easily separated and purified from disrupted magnetic bacteria by magnetic separation using a magnet. Each BMP has a single magnetic domain of magnetite and are well-dispersed in aqueous solutions because of the enclosing membrane.[5] On the basis of the above advantageous properties, BMPs have been utilized in fluoroimmunoassays,[5–7] mRNA recovery[8] and DNA carriers.[9] BMPs have vast potential for various technological applications and the molecular mechanism of their formation is of particular interest.

Our knowledge of the characteristics of BMPs has been gathered from our studies on the mechanism of magnetite particle formation in *Magnetospirillum magneticum* strain

Tadashi Matsunaga

Current Dean of Engineering at the Tokyo University of Agriculture and Technology. He has published numerous papers on the isolation of several key proteins and genes which provided important insights into the molecular events leading to magnetite synthesis in bacteria Magnetospirillum magneticum *strain AMB-1. He has also pioneered works on nanobiotechnological applications of bacterial magnetites, and in 2003, he was awarded an honorary degree of Doctor of Science from Heriot-Watt University in recognition of his distinguished academic career in biotechnology.*

Yoshiko Okamura

Research Fellow of the Japan Society for the Promotion of Science. Her research interest is in biomineralization. Her unique study has postulated on the biogenesis of bacterial magnetite membranes during magnetite formation. Her other work has provided an improved genetic transformation and expression systems for the magnetic bacterium M. magneticum *AMB-1.*

Tsuyoshi Tanaka

Assistant Professor at the Tokyo University of Agriculture and Technology. He studies the application of bacterial magnetites as magnetic carriers in diagnostic procedures such as immunoassays and DNA sensors. A fully automated analysis system using bacterial magnetites was developed through his contribution.

DOI: 10.1039/b404844j

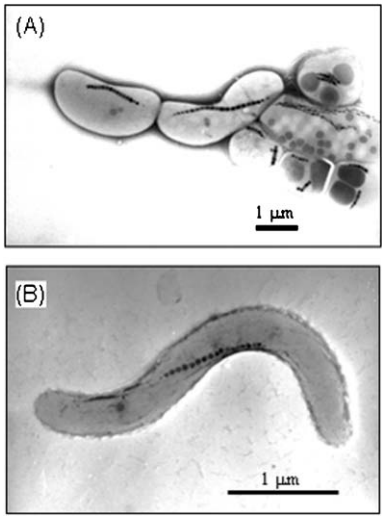

Fig. 1 Transmission electron microscope (TEM) images of magnetic bacteria. (A) Various magnetic bacteria collected by magnetic separation from freshwater sediment in Inokashira Park Musashino, Tokyo. (B) Magnetic bacterium, *Magnetospirillum magneticum* strain AMB-1.

AMB-1.[10] This review highlights the tremendous biotechnological potential of bacterial magnetite particles (BMPs) and our recent understanding of the mechanism of magnetite particle formation in *Magnetospirillum magneticum* strain AMB-1.

Bacterial magnetic particles

The morphology of BMP is varied and species-dependent. There are at least 3 kinds of BMP morphology identified: cubo-octahedron,[2] hexagonal prisms,[11] and elongated cubo-octahedron[12] (Fig. 2). Species-specific morphology suggests that genetic diversity and crystal growth controlling genes possibly exist. Although BMPs are commonly found in several species of magnetic bacteria in varying sizes ranging from 35 to 120 nm,[13–16] they maintain a single magnetic domain.

Bacterial magnetite particles can be distinguished from

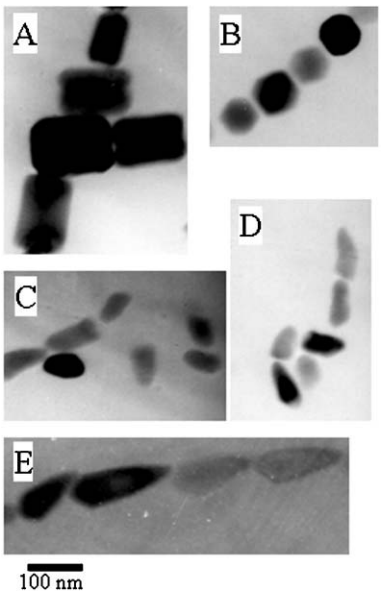

Fig. 2 TEM images of bacterial magnetic particles (BMPs) with different morphologies. (A) Cuboidal BMPs (cubo-octahedral morphology); (B) hexagonal BMPs; (C, D) Irregularly-shaped BMPs resembling elongated cubo-octahedral morphology; (E) bullet-shaped BMPs.

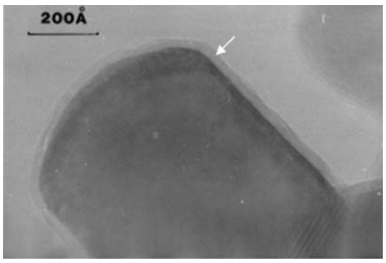

Fig. 3 TEM image of bacterial magnetic particles (BMPs) obtained from magnetic bacterium, *M. magneticum* AMB-1. The particle is surrounded by a membrane (arrow).

artificially synthesized magnetite by the presence of an organic membrane enveloping the particle as well as the regular morphology. Transmission electron microscopy (TEM) reveals that each BMP in a chain is encapsulated by a membrane approximately 2–4 nm in thickness (Fig. 3). The membrane contains 98% lipid and 2% other compounds. The lipid compounds in strain AMB-1 involve 58% phospholipids, which mainly consist of phosphatidylethanolamine.[5,16] The fatty acid components, which are similar to the cytoplasmic membrane of the cell, show three saturated (C12:0, C14:0) and two unsaturated fatty acids (C16:1, C18:1). Palmitoleic acid and oleic acid account for 90% of the total fatty acids. The phospholipids provide good dispersion of BMPs in aqueous solutions.[5] Other compounds include proteins incorporated into the BMP membrane. Until now, five proteins were shown to be specifically localized on the BMP membrane.[17,18] Species-specific morphology of magnetite in magnetic bacteria is considered to be controlled by these membrane proteins.

Mass production of bacterial magnetic particles

Pure cultivation of AMB-1 is one of the most important biotechnological processes in the application of BMPs. A magnetic bacterium, *M. magneticum* AMB-1, capable of growing aerobically has been successfully isolated.[19] In our initial work, mass scale cultivation in 1000 L has been done for the production of BMPs from which approximately 2.6 mg BMPs was yielded per liter of culture.[20] To enhance the productivity, high density cultivation of AMB-1 has been performed in a fed-batch culture system. In a batch culture of AMB-1, a final cell concentration of 1.8×10^8 cells ml^{-1} was obtained using a synthetic medium (magnetic sprillum growth medium).[21] In the fed batch culture, the cell concentration increased to 2.2×10^9 cells ml^{-1} by continuous addition of succinate and nitrate to the medium.[22] The productivity of BMPs reached 4.7 mg per liter of culture, which corresponded to 1.8 times higher than the productivity in batch culture. However, the yield of BMPs per cell was decreased.

AMB-1 has two respiration pathways to transfer electrons. One for aerobic growth using O_2 as the final electron acceptor induces no magnetite formation. The other uses nitrate as the terminal electron acceptor and therefore requires lower media redox potentials, which is favorable for magnetite formation. Therefore, oxygen control in cultivation of magnetic bacteria is a key factor for production of BMPs. To optimize the BMP production, high density cultivation under various oxygen concentrations in the gas phase was investigated. Limited oxygen in the gas phase enhanced cell growth with increasing BMP production.[23] Furthermore, ferrous sulfate and ferric gallate as iron sources dramatically enhanced BMP yield as compared with ferric quinate, an iron chelate conventionally used. The optimized conditions increased BMP production to 14.8 ± 0.5 mg dry weight per liter of culture, which corresponded to 5.7 times higher than the productivity in batch culture. The high density cultivation techniques of magnetic

bacteria have been applied to the production of genetically engineered BMPs by using a recombinant AMB-1.[24]

Magnetite formation regulated by membrane proteins

Several processes are involved in BMP synthesis, and one of the most important is the formation of vesicles consisting of lipids. It is hypothesized that the BMP membrane is derived from the cytoplasm through an invagination process.[18] To determine the mechanisms of magnetite formation, the isolation and characterization of the genes and proteins involved in the process have been undertaken in AMB-1. The *magA* gene, which shows homology to the Na^+/H^+ antiporter NapA,[25] was isolated in *M. magneticum* AMB-1 through transposon mutagenesis.[26] Intracellular localization of the MagA protein indicated that this protein is localized in both the cytoplasmic and BMP membranes.[27] Interestingly, MagA topology is inversely oriented between the cytoplasmic and the BMP membrane. MagA appears to function for iron efflux in the former and iron influx in the latter. To investigate the original function of MagA protein *in vivo*, the iron-uptake activity of MagA was determined using inverted vesicles prepared from fragmented membrane-expressing MagA protein in *E. coli* (Fig. 4). Addition of ATP initiated the accumulation of ferrous ions in the vesicles. The ions were released by the addition of protonophore. This activity was also observed under an artificial proton gradient without ATP. These results suggest that MagA protein is a proton-driving $H^+/Fe(II)$ antiporter.[28] MagA protein may play roles in transporting Fe^{2+} to the vesicle to grow up to BMPs and the alkalization of the inside of vesicles due to its $H^+/Fe(II)$ antiporter function. The size regulation of magnetite could be controlled by a coprecipitation of Fe(II) and Fe(III) *via* alkalization in the nano-sized vesicles in the same manner as a coprecipitation method *in vitro*.

Organic matrices were contained in biominerals which act as templates of crystallization and frameworks of crystals which associate with mineral surfaces and inhibit crystal growth. Many biominerals are elaborate and ingenious due to organic matrices. In order to isolate the regulation factors in the biosynthesis of magnetic particles, the proteins directly and tighly bound to BMPs were separated.[29] Four isolated proteins have the common sequence LGLGLGLGAWGPXXLGXXG-XAGA. Especially a 6 kDa protein, Mms6, deduced from the full length 399-bp gene is a 12.5 kDa premature polypeptide, however, the N-terminus of which obtained by Edman degradation starts at the 75 Gly. Mature Mms6 consisted of hydrophobic domain in the N-terminal region predicted as a transmembrane region by computer analysis, and a highly acidic domain, the C-terminal region of Mms6 was identified. Amino acids containing hydroxyl groups were also observed. Furthermore, the region between the middle and C-terminal regions contained basic amino acids such as Lys, Tyr, and Arg. These structural features were also observed in the other three isolated proteins, Mms5, Mms7, and Mms13.[29] The hydrophilic domains in mineral-associated proteins capture metal ions[30,31] or interact with the mineral phase.[32] Radioactive iron-binding experiments were performed with recombinant Mms6 corresponding to the mature protein produced in *E. coli*. Recombinant Mms6 showed obvious iron-binding activity. Addition of non-radioactive Fe^{3+} blocked the binding of radioactive Fe^{3+} to Mms6. Inhibition of binding of radioactive Fe^{3+} to Mms6 was also observed in the presence of Ca^{2+} and Mg^{2+}.[29] Following that, the effect of Mms6 on crystal formation was determined during synthesis of artificial magnetite. The magnetic precipitates with Mms6 showed cuboidal morphology with sizes ranging from 20 to 30 nm (Fig. 5). The results of electron diffraction analysis indicated that the

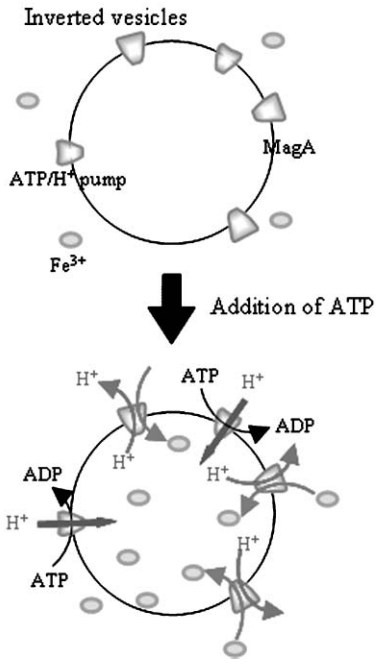

Fig. 4 Schematic diagram for iron transport through the MagA protein on inverted vesicles. Iron transport by MagA was verified by direct measurements of iron in MagA containing inverted-membrane vesicles.

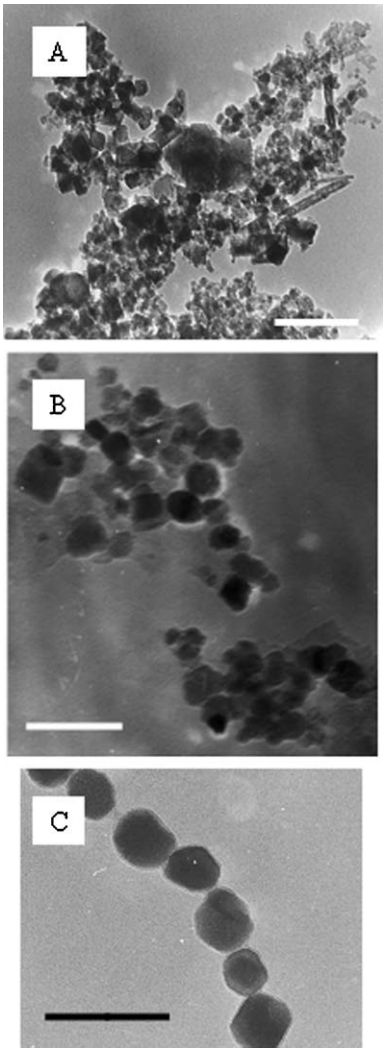

Fig. 5 TEM images of organically and inorganically synthesized magnetic particles. The magnetic iron precipitates were synthesized *in vitro* (A) without or (B) with coprecipitation with Mms6. (C) BMPs from *Magnetospirillum magneticum* strain AMB-1 extracts magnetically separated and washed by sonication. Bars indicate 100 nm.

black particles were composed mainly of magnetites. The shape of the precipitates was similar to that of BMPs synthesized by *M. magneticum* AMB-1 while the magnetic particles produced in the absence of Mms6 were non-homogeneous in size (1–100 nm) and shape. The observed needle-shaped crystals are similar to α-FeOOH.[29] These results suggest that Mms6 regulates crystallization, morphology and size by directly binding with ferric iron or magnetite.

Use of BMPs as drug carriers

BMPs show good dispersity in aqueous solutions, because the surface membrane, which mainly contains phosphatidyl-ethanolamine, is more negative in charge under conditions of low ionic strength and neutral pH.[33] The good dispersity of BMPs has led to the development of a novel magnetoliposome as a carrier in drug delivery system. BMPs were encapsulated in liposomes with well-dispersed conditions by the reverse-phase evaporation methods, while artificial magnetites aggregated in liposomes (Fig. 6).[34] The volume of captured drug in magneto-liposomes with BMPs was 1.7 times higher than in the ones with artificial magnetite particles. As a preliminary experiment, magnetoliposomes containing BMPs and FITC-labeled DNA were prepared for the investigation of the effect of a rotating magnetic field on the FITC-DNA released from magnetolipo-somes. FITC-DNA was not released from magnetoliposomes even after 2 h of incubation when a rotating magnetic field was not applied. When a rotating magnetic field was applied, however, the FITC-DNA released from the magnetoliposomes increased rapidly, becoming stationary after 2 h. This indicates that the application of an external magnetic field caused the magnetoliposomes to disrupt, releasing the FITC-DNA that was housed in the magnetoliposomes.

Antitumor activity against mouse squamous cell carcinoma (KLM205) was examined by using magnetoliposomes contain-ing *cis*-diamminedichloroplatinum (CDDP). Magnetic control of magnetoliposomes was utilized to concentrate drugs to specific targets. CDDP captured by magnetoliposomes with BMPs was added to 100 μl of cell culture (2 × 103 cells) of KLM205. An amount of 0.10 μg of CDDP with magnetolipo-somes and free CDDP affected 65% and 61% of cell growth inhibition, respectively.[34] The magnetoliposomes containing CDDP and free CDDP showed nearly equal growth inhibition effects on KLN205 cells *in vitro*.

Surface modification of BMPs by amino-silane for DNA extraction

DNA extraction is a fundamental procedure for molecular biological techniques, ranging from DNA sequence analysis to genetic recombination. The use of magnetic particles as a solid

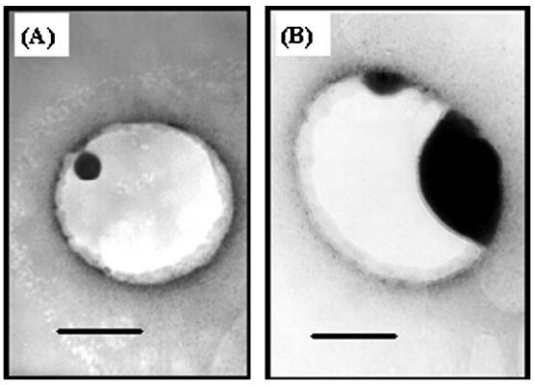

Fig. 6 TEM images of magnetoliposomes. (A) Liposome containing BMP; (B) liposome containing artificial magnetic particles. Bar indicates 100 nm.

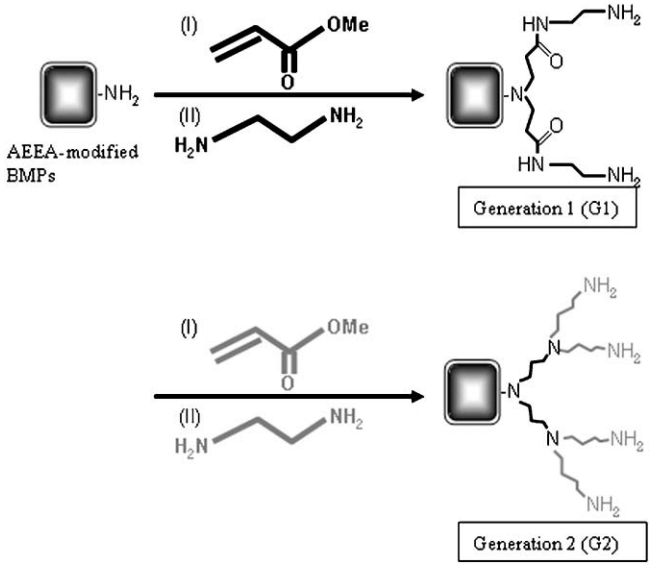

Fig. 7 Polyamidoamine dendrimer synthesis on the surface of amino silane modified BMPs. Dendrimer generation was initiated with AEEA coated BMPs in methylacrylate (I). Then, ethylenediamine (II) was reacted with the modified BMPs (Generation 1). Stepwise growth was repeated until the desired number of generations was achieved.

phase adsorbent is well suited for DNA extraction techniques, because they can be easily manipulated through simple application of a magnet. Although artificially synthesized iron oxide has the capacity to adsorb DNA,[35] aggregation is prominent due to magnetic attraction reducing the usable surface area. Initial application of native BMPs for this purpose revealed further modification was necessary. Organo-silane compounds can be covalently bound to iron oxides[36,37] introducing a positive ionic charge beneficial for restoring dispersion and facilitating ionic interactions between DNA. Use of 3-[2-(2-aminoethyl)-ethylamino]-propyltrimethoxysilane (AEEA)-modified BMPs resulted in appreciable increases in DNA extraction abilities. The DNA binding efficiency was 14 fold higher than untreated magnetite.[38] Moreover, BMPs were modified using a polyamidoamine (PAMAM) dendrimer to increase the number of amino groups.[39] A PAMAM dendrimer forms a dense outer amine shell through a cascade type of polymer generation (Fig. 7). Bacterial magnetic particles at successive dendrimer generations were investigated for DNA binding abilities (Table 1). The amine numbers double with every layer generated on the BMP surface. On the other hand, the number of amino groups generated on the same size of artificially synthesized magnetic particle is one tenth of that on the BMP at generation six. Modified magnetic particles were mixed with 25 μg of calf thymus DNA. The amount of DNA binding by dendrimer modified BMPs increased with every generation and 24.83 ± 1.61 μg of DNA bound to 100 μg bacterial magnetite at generation six. Furthermore, there was a linear correlation with the amount of DNA removed from solution and increased amino charge as dendrimer generations also increased. This occurrence further confirms the removal of DNA from solution is because of cationic charge contribution.

Table 1 Number of amines and amount of DNA on bacterial magnetic particle at different dendrimer generations

Generation	Amine number/BMP	μg DNA/100 μg magnetic particles
AEEA	2.1×10^4	3.59 ± 0.37
G1	6.8×10^4	4.43 ± 0.26
G3	2.6×10^4	5.89 ± 0.07
G5	1.1×10^4	11.95 ± 0.68
G6	1.7×10^4	24.83 ± 1.61

DNA recovery was obtained by incubating the DNA complex at 50 °C for 30 min resulting in 87% release (21.70 ± 1.59 μg). DNA recovery with dendrimer modified BMPs is about 6 times higher than with dendrimer modified artificial magnetic particles.[39]

Further modification of these magnetic particles using dendrimer technologies finally resulted in a product with desirable characteristics. Dendrimer modified magnetic particles suspend and disperse well in aqueous media, optimizing functional surface area. TEM images of modified bacterial magnetic particles indicate increased ionic repulsions at subsequent generations (Fig. 8). Initially the bacterial magnetic particles are seen as tight aggregates by TEM due to insufficient repulsive force between the magnetite (Fig. 8A). Generation three dendrimer modified magnetic particles were preferentially aligned in chains or tight aggregates (Fig. 8B). This phenomenon is likely a result of preferential particle alignment at the magnetic poles where magnetic moment is the strongest. The presence of a repulsive ionic charge that is strong enough to reduce non-magnetic pole alignments cause this to occur, similar to native bacterial magnetic particles containing membranes. At generation six ionic repulsions are strong enough to overcome magnetism and the dendrimer modified bacterial magnetic particles are visually disperse (Fig. 8C). A 4 nm layer surrounding the magnetite was observed (Fig. 8D). Recently, a DNA extraction procedure using dendrimer-modified BMPs has been successfully automated.[40]

Application of antibody-chemically conjugated to BMPs to immunoassays

BMPs possess lipid membranes with outward pointing amine groups. The amine groups have been used for immobilization of enzymes, antibodies and DNA. The use of magnetic particles as antibody carriers enables the separation of bound and free antigen by applying a magnetic field. Magnetic particles serve as both solid supports and as a means of separation in the assay system. Potentially larger surface areas on the particles may provide higher densities of antibodies on their surface. The amount of antibody coupling with BMPs was approximately 3 to 4 times higher than magnetite particles without membrane.[5] To maintain the functional properties of antibodies, various chemical conjugations of antibodies onto BMPs have been carried out by using homofunctional or heterofunctional reagents, such as glutaraldehyde, bis(sulfosuccinimidyl)suberate (BS3), succinimidyl 3-(2-pyridyldithio)propionate (SPDP) and/or succinimidyl 4-(*N*-maleimidomethyl)cyclohexane-1-carboxylate (SMCC) (Fig. 9).[5,7,41–43] Chemiluminescence and fluorescence immunoassays, which are divided into two distinct classes that are referred to as heterogeneous and homogeneous, have been developed based on sandwich and competitive inhibition formats. A sandwich chemiluminescence enzyme immunoassay using antibody-conjugated to BMPs permits the development of highly sensitive assays. Anti-mouse IgG antibody-BMPs

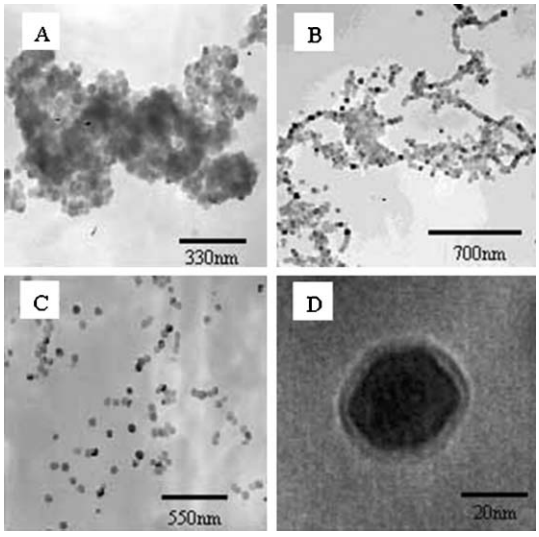

Fig. 8 TEM images of dendrimer modified BMPs when 20 μg ml^{-1} BMPs was applied and dried onto the mesh grids. A: AEEA coat, B: generation three, C and D: generation six.

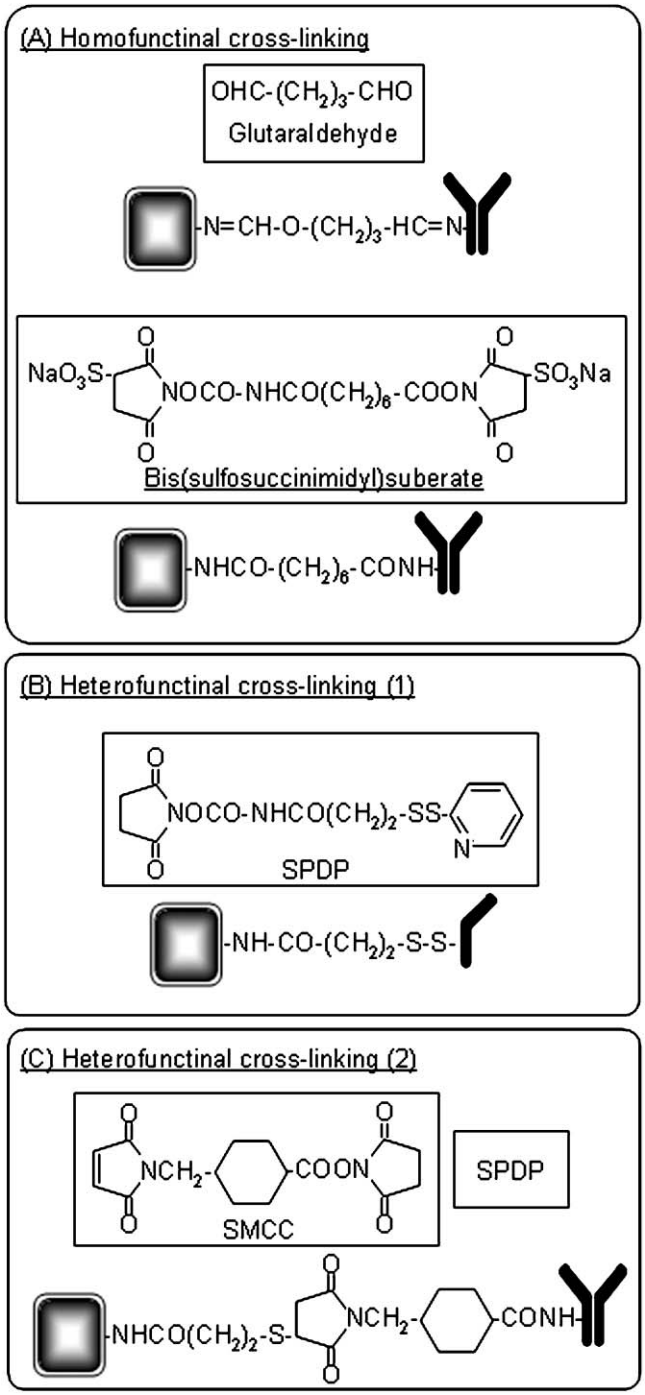

Fig. 9 Procedures for antibody-conjugation onto BMPs. (A) Homofunctional cross-linkers, which contain two aldehydes or two *N*-hydroxysuccinimide (NHS) esters reacted with amines on BMPs and antibodies, were used for their covalent binding. (B) A heterofunctional cross-linker, SPDP, which contains one NHS ester, was used for the thiolation of BMPs. Dithiothreitol was reacted with antibodies for the reduction. (C) Two heterofunctional cross-linker were used for preservation of antibody specificity after chemical conjugation. SMCC, which contains NHS-ester and maleimide, were reacted with antibodies.

prepared by SPDP and SMCC and alkaline phosphatase (ALP)-conjugated anti-mouse IgG secondary antibody were used for the detection of mouse IgG. A good correlation was obtained between the luminescence intensity and mouse IgG concentration in the range of 1 to 10^5 fg ml^{-1}. The minimum detectable concentration of IgG is 1 fg ml^{-1} (corresponding to 6.7 zmol = 4000 molecules ml^{-1} as calculated from Avogadro's number).[41]

Furthermore, competitive chemiluminescence enzyme immunoassays using antibody-conjugated onto BMPs allow the rapid and sensitive detection of small molecules, such as environmental pollutants, hormone and toxic detergents.[42,43] Xenoestrongens, such as alkylphenol ethoxylates (APE), bisphenol A (BPA) and linear alkylbenzene sulfonates (LAS) were detectable using monoclonal antibodies conjugated onto BMPs based on the competitive reaction of xenoestrongens and ALP-conjugated xenoestrongens.[42] The entire procedure was completed in 15 min while typical plate methods took more than 2.5 h. This method gave a wider range and lower detection limit than ELISA in which the same antibodies were used for detection. Furthermore, detection limits of LAS and BPA were at similar levels compared with those obtained through GC-MS or LC-MS. These experiments suggest that BMP-based immunoassay systems have superior advantages due to the high sensitivity and rapid measurement of samples.

Design of genetically engineered BMPs for immuno and receptor assay

The Z-domain of protein A in *Staphylococcus aureus* has the binding ability to the Fc region of IgG.[44] An assembly technique of the Z-domain on the BMP surface by gene fusion using a *protein A–magA* hybrid gene have been constructed (Fig. 10A). MagA protein acts as an anchor for the site-specific assembly of functional foreign proteins.[45] Antibody was accurately oriented on BMPs due to its association with protein A unlike when immobilization by chemical conjugation was employed. When a chemiluminescence enzyme immunoassay was carried out using antibody–protein A–BMP complexes and BMPs chemically conjugated to antibodies, the antigen binding activity per microgram of antibodies on antibody–protein A-BMP complexes was two times higher than that for antibody–BMP conjugates prepared by chemical conjugation.[33] A sensitive immunoassay for the detection of human IgG[45] has been developed using antibody–proteinA–BMP complexes.

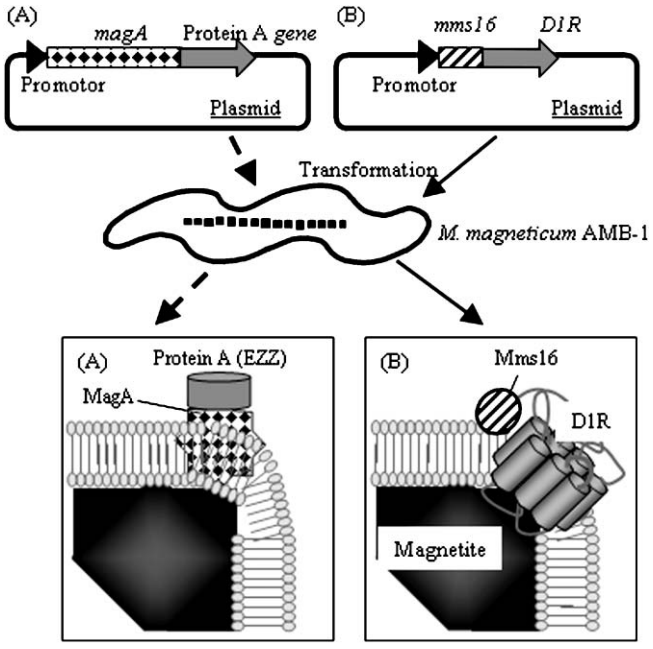

Fig. 10 Schematic diagram for preparation of recombinant BMPs assembled protein A and D1R. Plasmid containing a fusion gene of *magA* and protein A (Z-domain) gene (pEZZM) (A) or a fusion gene of *mms16* and D1R gene (pUM16D1) (B) were transformed into wild-type AMB-1.

Another anchoring membrane protein, Mms16,[18] was examined for assembling membrane protein since it allows protein folding (Fig. 10B).[46] G-protein coupled receptors (GPCRs) are the most abundant class of receptors in mammalian biology. Operating by way of their linked signaling pathways, they participate in a myriad of biological processes. Because of their pivotal role in physiology, these receptors are the major focus of pharmaceutical drug development. In general, comparative binding assay is applied for ligand detection. GPCR (D1 dopamine receptor) maintains the ligand-binding ability on BMP membrane using Mms16 as anchor. D1 dopamine receptor was displayed with affinity for the antagonist [^{3}H]SCH23390, with a *Kd* value of 9.7 nM. This *Kd* is similar to the value obtained from Sf9 cells using the baculovirus expression vector system (*Kd* = 2.4 nM). This detection system was able to quantify the amount of ligands.[46]

Automation of BMP-based immunoassay

In developing a biosensor, the words fast, reliable and precise as well as sensitive, are used to describe required elements. Automated assay systems allow the development of precise, reliable and fast assays. Until now, automated immunoassay systems using BMPs have been examined to detect various biological markers.[33,42,43,47] A fully automated immunoassay system is equipped with a reaction station with a 96-well microtiter plate, a tip track, multi-pipets, a magnetic separation unit and a luminescence detection unit. Genetically engineered BMPs, protein A–BMP complexes have been applied to the fully automated immunoassay system for the detection of human insulin from blood. Dose response curves were obtained from the luminescence intensity for human insulin concentration in serum. A detection limit of 2 μU ml^{-1} of human insulin and a linear correlation between luminescence intensity and concentration was obtained over the range of 19–254 μU ml^{-1}.[33] The correlation of results for insulin (Enzymum Test Insulin) was investigated. Linear regression analysis yielded a correlation coefficient of 0.999 and a slope of 0.99 for methods using automatic procedures.

Application of automated BMP-based assay to SNPs analysis

Furthermore, an automated workstation for BMP-based single nucleotide polymorphisms (SNPs) discrimination has been designed. SNPs are the most common of human genotype variations. In molecular epidemiology studies, susceptibility between disease and gene is analyzed from a statistical viewpoint. Therefore, multiple samples are necessary to analyze. The designed workstation is equipped with a 96-way automated pipetter which collects and dispenses fluids as it moves in *x*- and *z*-directions. The platform contains a disposable tip rack station, a reagent vessel and a reaction station for a 96-well microtiter plate. BMPs were collected by attaching a neodymium iron boron sintered (Nd-Fe-B) magnet on the bottom of the microtiter plate. This system permits the simultaneous heating and magnetic separation of 96 samples per assay. The principle for SNP discrimination using BMPs is based on fluorescence resonance energy transfer (FRET) between FITC (donor) and POPO-3 (acceptor) bound to double-stranded DNA[48,49] or DNA thermal dissociation curve analysis.[50] A detection system for the discrimination of SNP in aldehyde dehydrogenase 2 (ALDH2) gene and transforming growth

factor-β1 (TGF-β1) gene has been developed. SNP in ALDH2 gene on chromosome 12 has significant implications in the evaluation of susceptibility of human organs to damage induced by alcohol.[51] TGF-β1 is commonly associated with a $T^{869} \rightarrow C$ ($Leu^{10} \rightarrow Pro$) polymorphism and is a genetic marker for osteoporosis susceptibility.[52] These assays described in this study allow a high throughput discrimination of SNPs.

Conclusion

Nanoscale and molecular engineered BMPs have been developed for many engineering applications by chemical processes and genetic manipulation techniques. Improved analysis and identification of BMP specific factors will facilitate the use of BMPs as a biomimetic technique for *in vitro* production of highly controlled nanocrystals. Especially, *in vitro* synthesis of magnetoliposome using Mms6, which provides nucleation sites for precipitation of iron oxide in the vesicle, will give much information to control the crystal size and morphology. These studies will potentially bring several interesting findings, such as site-specific immobilization of useful protein on magnetite crystals, and quantum-size-effects in magnetic particles with well-controlled size and shape.

Although BMP formation has been extensively examined at the molecular level, further studies are still required to elucidate the whole mechanism of this highly controlled biomineralization process. Recent progress in molecular biology will facilitate more highly organized and systematic studies towards this goal. Recently, comparative genome analysis of magnetic bacteria between genera or species has been launched to perform genome-wide screening of genes related to BMP formation. Furthermore, gene mapping by using transposon mutants will refine our search from genome-wide screening. In parallel, comprehensive analysis of specific proteins on BMP membrane has been proceeded by shotgun proteomics.

References

1 R. B. Frankel, R. P. Blakemore and R. S. Wolfe, *Science*, 1979, **203**, 1355.
2 S. Mann, R. B. Frankel and R. P. Blakemore, *Nature*, 1984, **310**, 405.
3 T. Sakaguchi, J. G. Burgess and T. Matsunaga, *Nature (London)*, 1993, **365**, 47.
4 D. A. Bazylinski, *Int. Microbiol.*, 1999, **2**, 71.
5 N. Nakamura and T. Matsunaga, *Anal. Chim. Acta*, 1993, **281**, 585.
6 N. Nakamura, K. Hashimoto and T. Matsunaga, *Anal. Chem.*, 1991, **63**, 268.
7 N. Nakamura, J. G. Burgess, K. Yagiuda, S. Kudo, T. Sakaguchi and T. Matsunaga, *Anal. Chem.*, 1993, **65**, 2036.
8 K. Sode, S. Kudo, T. Sakaguchi, N. Nakamura and T. Matsunaga, *Biotechnol. Techniques*, 1993, **7**, 688.
9 H. Takeyama, A. Yamazawa, C. Nakamura and T. Matsunaga, *Biotechnol. Techniques*, 1995, **9**, 355.
10 T. Matsunaga and Y. Okamura, *Trends Microbiol.*, 2003, **11**, 536.
11 T. Matsuda, J. Endo, N. Osakabe, A. Tonomura and T. Arii, *Nature*, 1983, **302**, 411.
12 S. Mann, N. H. C. Sparks and R. Blakemore, *Proc. R. Soc. London*, 1987, **B231**, 477.
13 D. A. Bazylinski, A. J. Garratt-Reed and R. B. Frankel, *Microsc. Res. Technol.*, 1994, **27**, 389.
14 R. B. Frankel and D. A. Bazylinski, *Hyperfine Interact.*, 1994, **90**, 135.
15 B. M. Moskowitz, *Rev. Geophys. Suppl.*, 1995, **33**, 123.
16 R. B. Frankel, D. A. Bazylinski and D. Schueler, *Supramol. Sci.*, 1998, **5**, 383.
17 Y. Okamura, H. Takeyama and T. Matsunaga, *Appl. Biochem. Biotechnol.*, 2000, **84–86**, 441.
18 Y. Okamura, H. Takeyama and T. Matsunaga, *J. Biol. Chem.*, 2001, **276**, 48183.
19 T. Matsunaga and S. Kamiya, *Appl. Microbiol. Biotechnol.*, 1987, **26**, 328.
20 T. Matsunaga, F. Tadokoro and N. Nakamura, *IEEE Trans. Magn.*, 1990, **26**, 1557.
21 R. P. Blakemore, D. Maratea and R. S. Wolfe, *J. Bacteriol.*, 1979, **140**, 720.
22 T. Matsunaga, N. Tsujimura and S. Kamiya, *Biotechnol. Techniques*, 1996, **10**, 495.
23 C. Yang, H. Takeyama, T. Tanaka and T. Matsunaga, *Enzyme Microbial Technol.*, 2001, **29**, 13.
24 T. Matsunaga, H. Togo, T. Kikuchi and T. Tanaka, *Biotechnol. Bioeng.*, 2000, **70**, 704.
25 M. Waser, D. Hess-Bienz, K. Davies and M. Solioz, *J. Biol. Chem.*, 1992, **267**, 5396.
26 T. Matsunaga, C. Nakamura, J. G. Burgess and K. Sode, *J. Bacteriol.*, 1992, **174**, 2748.
27 C. Nakamura, T. Kikuchi, J. G. Burgess and T. Matsunaga, *J. Biochem. (Tokyo)*, 1995, **118**, 23.
28 C. Nakamura, J. G. Burgess, K. Sode and T. Matsunaga, *J. Biol. Chem.*, 1995, **270**, 28392.
29 A. Arakaki, J. Webb and T. Matsunaga, *J. Biol. Chem.*, 2003, **278**, 8745.
30 S. J. Hattan, T. M. Laue and N. D. Chasteen, *J. Biol. Chem.*, 2001, **276**, 4461.
31 S. J. Lippard and J. M. Berg, *Principles of Bioinorganic Chemistry*, University Science Books, Mill Valley, CA, 1994.
32 P. A. Raj, M. Johnsson, M. J. Levine and G. H. Nancollas, *J. Biol. Chem.*, 1992, **267**, 5968.
33 T. Tanaka and T. Matsunaga, *Anal. Chem.*, 2000, **72**, 3518.
34 T. Matsunaga, Y. Higashi and N. Tsujimura, *Cellular Eng.*, 1997, **2**, 7.
35 M. J. Davies, J. I. Taylor, N. Sachsinger and I. J. Bruce, *Anal. Biochem.*, 1998, **262**, 92.
36 C. W. Jung, *Magn. Reson. Imaging*, 1995, **13**, 675.
37 H. Kobayashi and T. Matsunaga, *J. Colloid Interface Sci.*, 1991, **141**, 505.
38 B. Yoza, M. Matsumoto and T. Matsunaga, *J. Biotechnol.*, 2002, **94**, 217.
39 B. Yoza, A. Arakaki and T. Matsunaga, *J. Biotechnol.*, 2003, **101**, 219.
40 B. Yoza, A. Arakaki, K. Maruyama, H. Takeyama and T. Matsunaga, *J. Biosci. Bioeng.*, 2003, **95**, 21.
41 T. Matsunaga, M. Kawasaki, X. Yu, N. Tsujimura and N. Nakamura, *Anal. Chem.*, 1996, **68**, 3551.
42 T. Matsunaga, F. Ueki, K. Obata, H. Tajima, T. Tanaka, H. Takeyama, Y. Goda and S. Fujimoto, *Anal. Chim. Acta*, 2003, **475**, 75.
43 T. Tanaka, H. Takeda, F. Ueki, K. Obata, H. Tajima, H. Takeyama, Y. Goda, S. Fujimoto and T. Matsunaga, *J. Biotechnol.*, 2004, **108**, 153.
44 B. Lowenadler, B. Jansson, S. Paleus, E. Holmgren, B. Nilsson, T. Moks, G. Palm, S. Josephson, L. Philipson and M. Uhlen, *Gene*, 1987, **58**, 87.
45 T. Matsunaga, R. Sato, S. Kamiya, T. Tanaka and H. Takeyama, *J. Magn. Magn. Mater.*, 1999, **194**, 126.
46 T. Yoshino, M. Takahashi, H. Takeyama, Y. Okamura, F. Kato and T. Matsunaga, *Appl. Environ. Microbiol.*, 2004, **70**, 2880.
47 T. Tanaka and T. Matsunaga, *Biosens. Bioelectron.*, 2001, **16**, 1089.
48 H. Nakayama, A. Arakaki, K. Maruyama, H. Takeyama and T. Matsunaga, *Biotechnol. Bioeng.*, 2003, **84**, 96.
49 T. Tanaka, K. Maruyama, K. Yoda, E. Nemoto, Y. Udagawa, H. Nakayama, H. Takeyama and T. Matsunaga, *Biosens. Bioelectron.*, 2003, **19**, 325.
50 K. Maruyama, H. Takeyama, E. Nemoto, T. Tanaka, K. Yoda and T. Matsunaga, *Biotechnol. Bioeng.*, in press.
51 W. J. Chen, E. W. Loh, Y. P. Hsu and A. T. Cheng, *Biol. Psychiatry*, 1997, **41**, 703.
52 Y. Yamada, *Mech. Ageing Dev.*, 2000, **116**, 113.